

Numerical study on thin plates under the combined action of shear and tensile stresses

S. Sathiyaseelan^a and K. Baskar*

Department of Civil Engineering, National Institute of Technology, Trichy-620015, India

(Received February 17, 2011, Revised April 18, 2012, Accepted May 17, 2012)

Abstract. Analytical (Rayleigh-Ritz method) and numerical studies are carried out and buckling interaction curves are developed for simply supported plates of varying aspect ratios ranging from 1 to 5, under the combined action of in-plane shear and tension. A multi-step buckling procedure is employed in the Finite Element (FE) model instead of a regular single step analysis in view of obtaining the buckling load under the combined forces. Both the analytical (classical) and FE studies confirm the delayed shear buckling characteristics of thin plate under the combined action of shear and tension. The interaction curves are found to be linear and are found to vary with plate aspect ratio. The interaction curve developed using Rayleigh-Ritz method is found to deviate in an increasing trend from that of validated FE model as plate aspect ratio is increased beyond value of 1. It is found that the observed deviation is due to the insufficient number of terms that is been considered in the assumed deflection function of Rayleigh-Ritz method and a convergence study is suggested as a solution.

Keywords: plate; shear; tension; buckling; Rayleigh Ritz; FEM; in-plane; interaction; classical solution; numerical study

1. Introduction

A plate can be considered as a thin plate if the thickness to the least lateral dimension ratio is less than 0.05 (Chandrashekhara 2001). Thin plates with and without perforations do exist in many structures and structural components such as plate girders, ship structures, aerospace structures etc. In such cases, the plates are subjected to various in-plane load combinations, which make it to undergo form failure i.e., buckling mode of failure. Hence, in order to have a reliable design, the buckling load is to be determined for each load combination that is getting generated in the given field condition. This led to the development of elastic buckling solution for thin plates subjected to various in-plane load combinations, under various boundary conditions. Though research in the area of thin plate buckling started since early 1940's, most of the study that undertaken since 1980's concentrated on perforated plates, with un-perforated case not given a detail investigation. Detailed literature review on perforated plates subjected to various in-plane loads/load combinations can be found in research papers of Brown and Yettram (1986), Brown *et al.* (1987), Pellegrino *et al.*

*Corresponding author, Associate Professor, E-mail: drkbaskar@yahoo.co.in

^aResearch Scholar, E-mail: sathiyaseelann.s@gmail.com

(2009), Maiorana *et al.* (2009), Moen and Schafer (2009), Narayanan *et al.* (1984), Paik (2007), Sawy and Nazmy (2001), Sawy and Martini (2007), Shimizu (2007), Yettram and Brown (1985, 1986). The studies that had been well developed on the linear buckling behavior of un-perforated thin plates are mostly confined to following standard cases.

Studies related to un-perforated Plates: Timoshenko and Gere (1985) employed the equilibrium approach to study the behavior of thin plate subjected to in-plane compression. Conservation of energy using Fourier series was used to find the critical buckling load under biaxial compression/tension whereas, in the case of combined shear & bending and combined shear & compression, Rayleigh-Ritz method were used by Bulson (1970). Pure shear was treated using principle of minimum potential energy by Iyengar (1986). In the above cases, the change in buckling solution with respect to different boundary conditions such as simply supported, clamped, elastically restrained and their combination were investigated. In addition to above mentioned classical solution, considerable amount of research works involving either FEM or closed form formulations or other numerical approach have been carried out in recent past. Most of these research works predicts the buckling behavior of un-perforated thin plate subjected to one of the load cases which includes uniaxial compression, biaxial compression, direct shear, shear and direct stresses (axial compression/tension), bending or plate subjected to various combinations of some of the above mentioned load cases. These research works can be found in the papers of Alinia *et al.* (2009), Chen *et al.* (2009), Paik and Thayamballi (2000), Jaberzadeh and Azhari (2009), Lee *et al.* (1996), McKenzie (1963), Shahabian and Roberts (1999), Stowell and Schwartz (1943), Xiang *et al.* (2003).

Hence, numbers of studies have been carried out on elastic buckling behavior of un-perforated thin (Kirchhoff) plates, considering the different combinations of in-plane load in each case. Among the various load combinations, the study with respect to the combined action of shear and axial tension is limited and is not investigated in detail. But, the recent advancement in engineering applications leads the plates to the combined action of shear and tension which in turn induces the buckling in plate once the critical load combination is reached. As an example, the web of steel-concrete composite plate girder with its neutral axis lies within the concrete slab as shown in Fig. 1 is subjected to combined in-plane shear and axial tension (Baskar and Shanmugam 2003). Stowell and Schwartz (1943) indicated that the lower surface of an aircraft wings is usually subjected to

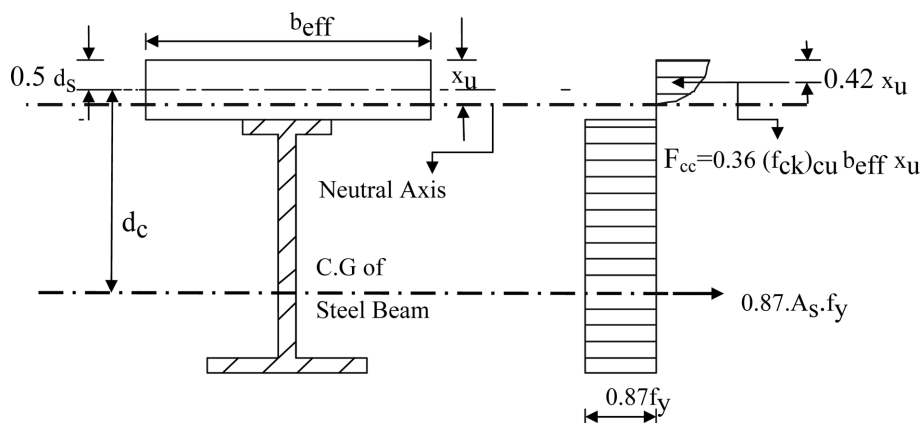


Fig. 1 Stress distribution in a composite plate girder with neutral axis lies within concrete slab (Source : IS 11384: 1985)

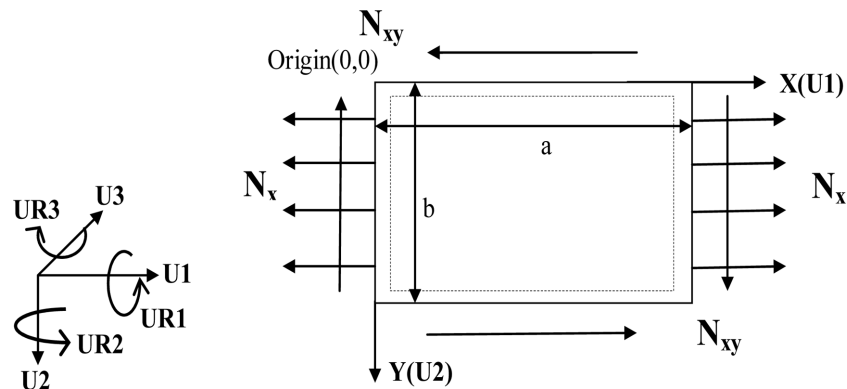


Fig. 2 Schematic diagram of plate under combined in-plane shear (N_{xy}) and tension (N_x)

combined action of shear and tension. These kinds of applications necessitate the buckling study on plates under the combined action of in-plane shear and tension and this formed the primary motivation for the present study area.

2. Problem definition

The formulation of elastic buckling interaction curve (Through both analytical and numerical modeling) for thin, homogeneous, isotropic steel plate subjected to combined action of in-plane shear and tension (see Fig. 2) is considered. Simply supported (out of plane) boundary condition is considered at all plate edges and plate aspect ratio ranging from 1 to 5 is considered as parameter.

3. Method of analysis

Two different analysis procedures such as classical closed form solution and Finite Element Analysis have been employed to predict the buckling behavior. As conventional equilibrium approach is not suitable for obtaining the solution (Iyengar 1986), the energy (Rayleigh-Ritz) approach is employed in the present study to obtain the solution for plates under the action of combined in-plane shear and tension. In the FE procedure, model is developed using general purpose FE software ABAQUS and is subjected to investigation. The buckling analysis is carried out with ABAQUS- Shell Finite Element Eigen Buckling Analysis and the results, in the form of normalized buckling interaction curve, are compared with that of classical method. In the numerical model, a new multistep buckling analysis procedure is proposed for resolving the constraint that exists for case of combined loading condition, in the conventional single step buckling analysis of ABAQUS.

4. Classical solution

Non dimensional forms of equations are used in the formulation in order to have simplified

integral computations (Iyengar 1986). Rayleigh-Ritz (energy) method is used for the buckling analysis and the interaction curves are drawn for plates of different aspect ratio ranging from 1 to 5. Thin plate theory and its assumptions are considered in the formulation of buckling solution.

4.1 Rayleigh-Ritz solution

4.1.1 Displacement function, $w(x, y)$

The deflection function representing the buckled i.e., slightly bent shape at bifurcation point is assumed and is shown in Eq. (1)

$$w = \sum_{m=1}^{\alpha} \sum_{n=1}^{\alpha} \left(A_{mn} \sin \frac{m\pi x}{a} \sin \frac{n\pi y}{b} \right) \quad (1)$$

The above displacement function is chosen since it satisfies all the required geometric boundary conditions. The non dimensional form of Eq. (1) is as follows

$$w = \sum_{m=1}^{\alpha} \sum_{n=1}^{\alpha} (A_{mn} \sin m\pi\xi \sin n\pi\eta) \quad (2)$$

Where,

$$\xi = \frac{x}{a} \quad \text{and} \quad \eta = \frac{y}{b}$$

4.1.2 Bending strain energy of the plate (U)

With the Kirchhoff hypothesis taken into consideration (Chandrashekhara 2001), the Strain Energy (U) of the loaded plate after substituting the expression for $w(x, y)$ is obtained as follows.

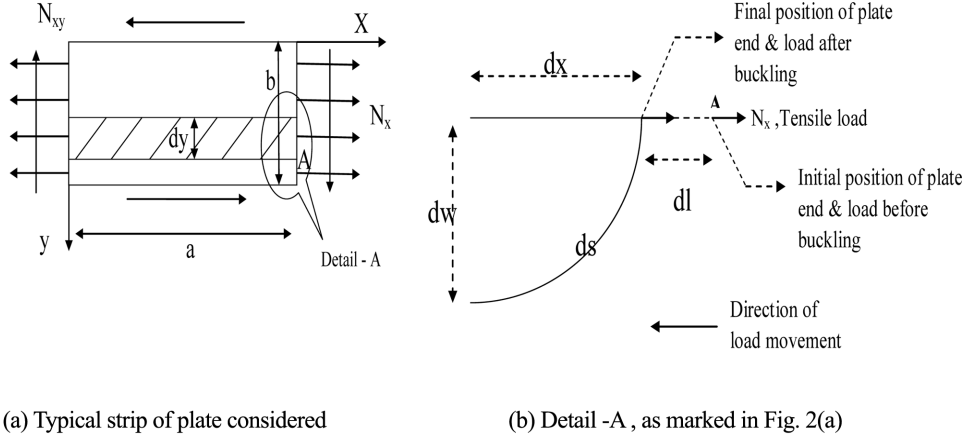
$$U = \left(\frac{D\pi^4}{8pa^2} \right) \sum_{m=1}^{\infty} \sum_{n=1}^{\infty} (A_{mn}^2 (m^2 + p^2 n^2)^2) \quad (3)$$

4.1.3 Potential energy due to external load system, V_e

4.1.3.1 Potential energy due to in – plane tension (N_x)

It is considered in the present study that buckling under combined shear and tension is essentially a ‘delayed shear buckling’, which means that plate buckling with its buckling mode shape same as that of pure shear case but relatively at higher shear load for the chosen plate system in the presence of given tensile force. This consideration of delayed shear buckling is also reported in literature as experimental observation (Baskar and Shanmugam 2003). As a result of this assumption, the tensile load movement during buckling will be opposite to its line of action. It is due to this phenomenon, the potential energy due to tension becomes additive in nature to plate strain energy, which in turn results in higher shear load at buckling (see Figs. 8, 9) when compared to that of pure shear condition for the given plate system. This phenomenon of shear buckling at an increased shear load for the given plate system, is mentioned in this report as ‘delayed shear buckling’. The results of numerical modeling of thin plate subjected to shear and tension (presented in sec. 6) confirmed this phenomenon of delayed shear buckling.

As the neutral plane of the plate is considered inextensible owing to the small deflection assumption of Kirchhoff’s hypothesis, the displacement (dl) of the edge due to in – plane tensile



(a) Typical strip of plate considered

(b) Detail -A, as marked in Fig. 2(a)

Fig. 3 Position of load before & after plate buckling

load, N_x over an element is equal to difference in length of deflection curve, ds and the length of the chord, dx connecting the loaded edges of the element. The same is illustrated in the Fig. 3. From Fig. 3(b), the potential energy due to tension (N_x) is derived as follows

$$dV_1 = -((-N_x) \cdot dy) \frac{1}{2} \int_0^a \left(\frac{dw}{dx} \right)^2 dx \quad (4)$$

Here, the outmost minus sign is due to definition of potential energy and inner minus is because of the fact that the directions of load and its movement during buckling is of opposite in nature. Hence, for the entire plate surface, after having substituted the expression for $w(x, y)$, the potential energy due to tensile load (V_1) is obtained as follows

$$V_1 = \left(\left(\frac{1}{8p} \right) \cdot N_x \cdot \pi^2 \sum_{m=1}^{\infty} \sum_{n=1}^{\infty} A_{mn}^2 m^2 \right) \quad (5)$$

Similarly, the potential energy due to in-plane shear is derived as follows

$$V_2 = \left((-4N_{xy}) \sum_{m=1}^{\infty} \sum_{n=1}^{\infty} \sum_{r=1}^{\infty} \sum_{s=1}^{\infty} \frac{A_{mn} \cdot A_{rs} \cdot mnrs}{(m^2 - r^2)(s^2 - n^2)} \right) \quad (6)$$

4.1.4 Total potential energy of the system, π

The total potential energy of the system is the sum of elastic potential energy, due to bending and potential energy of the external load system. It can be written in the following form

$$\pi = U + V_1 + V_2 \quad (7)$$

By principle of minimum potential energy, at buckling, we have

$$\frac{\partial \pi}{\partial A_{ij}} = 0 \quad (8)$$

Where, A_{ij} , $i, j = 1, 2, \dots, n$. denotes the constants of deflection function, $w(x, y)$. Since in stability analysis, bent configuration is of interest at buckling condition, a non trivial solution is needed i.e., determinant of matrix form of Eq. (8) should be zero and is shown below.

$$\begin{bmatrix} \frac{\pi^2}{4p} \left(N_x + \left(\frac{D\pi^2}{a^2} \cdot (1+p^2)^2 \right) \right) & 0 & 0 & \frac{32}{9} N_{xy} \\ 0 & \frac{\pi^2}{4p} \left(N_x + \left(\frac{D\pi^2}{a^2} \cdot (1+4p^2)^2 \right) \right) & -\frac{32}{9} N_{xy} & 0 \\ 0 & -\frac{32}{9} N_{xy} & \frac{\pi^2}{4p} \left(4N_x + \left(\frac{D\pi^2}{a^2} \cdot (4+p^2)^2 \right) \right) & 0 \\ \frac{32}{9} N_{xy} & 0 & 0 & \frac{\pi^2}{4p} \left(4N_x + \left(\frac{D\pi^2}{a^2} \cdot (4+4p^2)^2 \right) \right) \end{bmatrix} = 0$$

Here, only first few terms of the deflection function (corresponding to $m = n = r = s = 1, 2$) $w(x, y)$, is considered to arrive at the determinant owing to difficulty involved in solving with higher number of terms been considered in the approximating polynomial, $w(x, y)$. The determinant is solved for N_{xy} by substituting different combination of values for rest of the parameters and the interaction curves are generated with tensile (N_x) load in X -axis and the calculated shear (N_{xy}) in Y -axis. But in this way, many curves needs to be drawn corresponding to different values of b/t ratio and plate width (b), for each plate aspect ratio (p). Hence in order reduce the complexity, during each numerical substitution for b/t , b , p , N_x , corresponding critical shear buckling load, $N_{xy,cr}$ (i.e., buckling load of plate under pure shear) and compression buckling load, $N_{1x,cr}$ (i.e., buckling load of plate under pure compression) are calculated in addition to N_{xy} . The curves are then drawn with X -axis parameter as ratio of tensile load (N_x) to its corresponding $N_{1x,cr}$ and Y -axis parameter as ratio of calculated shear load at buckling, N_{xy} to its corresponding $N_{xy,cr}$. This normalization of X and Y axis parameter resulted in the convergence of curves corresponding to different b/t ratio and plate width (b) into a single normalized buckling interaction curve, for the case of each plate aspect ratio (p) and is shown in Figs. 8, 9.

5. Numerical (finite element) modeling

5.1 Buckling formulation-basis

The Numerical modeling of thin plates subjected to combined shear and tension is developed using ABAQUS - Shell Finite Element Eigen Buckling Analysis. In the Eigen Buckling analysis, the following stiffness formulation is used to arrive at Eigen value. Eigen value is then used to obtain the buckling load using the Eq. (10).

Stiffness Formulation

$$(K_o^{MN} + \lambda_i K_{\Delta}^{NM}) v_i^M = 0 \quad (9)$$

Where,

k_o^{MN} is the stiffness matrix corresponding to the base state, which includes the effects of the preloads, P^N if any.

k_{Δ}^{MN} is the differential initial stress and load stiffness matrix due to the incremental loading pattern, Q^N given in the buckling analysis step.

λ_i are the Eigen values.

V_i are the buckling mode shapes (eigenvectors).

M and N are degrees of freedom of the whole plate model.

The buckling load is given by

$$P^N + \lambda_i Q^N \tag{10}$$

In the present study, $P^N = 0$ in all the cases and hence buckling load is the product of eigen value and the applied load in BUCKLE step of ABAQUS.

5.2 FE Model (Procedure) description

5.2.1 Geometrical modeling of thin plate

Since, it is observed from the classical buckling solution (Figs. 8, 9) that the normalized buckling interaction curve depends only on plate aspect ratio and is independent of plate b/t ratio and plate width (b), steel plate of width 1 m and with thickness of .006 m (i.e., $b/t = 166$) is considered throughout the FE modeling of plates of different plate aspect ratio (1 to 5).

5.2.2 Method of buckling analysis

In the conventional single step buckling analysis through ABAQUS-BUCKLE step, the eigen value obtained represents the common factor (λ) of applied loads i.e., Q^N and hence it is not possible to obtain a value for one load at buckling for the given value of other load i.e., In case shear and tension, it is not possible to get the shear load at buckling for the given tensile load. Since it is not possible to develop a buckling interaction curve for combined loading case with this constraint in single step buckling analysis, a multistep buckling is proposed in the present study, in which tension is given in ABAQUS-GENERAL STATIC step and the shear is given in ABAQUS-BUCKLE step. Since in ABAQUS, the base state for the current step is the state (stress, strain, etc.) of model at the end of previous step, by adopting multistep buckling analysis, instability analysis is carried on the deformed plate model instead of un-deformed plate model itself.

5.2.3 Loading procedure

In this, the plate model is loaded using shell edge load – Normal edge traction(option in ABAQUS for applying edge line load) for tensile/compressive load and by shell edge load – shear edge traction (option in ABAQUS for applying plate edge shear) for shear load, by selecting the respective geometric edges as a load application area. The unit for both the load is Newton/mm width of plate edge.

5.2.4 Boundary condition

Since, rectangular plate loaded with a constant shear stress is not in moment equilibrium about the 3-axis i.e., Z-axis (Fig. 2), special attention is required when applying the boundary conditions to prevent rigid body rotation in the finite element model (Naik and Meon 2009). It is found through rigid body movement analysis that rigid body movement of plate model can be prevented by arresting either in-plane rotational Degrees of Freedom (DOF), UR3 (see Fig. 2) or in-plane translational DOF, U2 (see Fig. 2) or both. It is also found that buckling solution remains

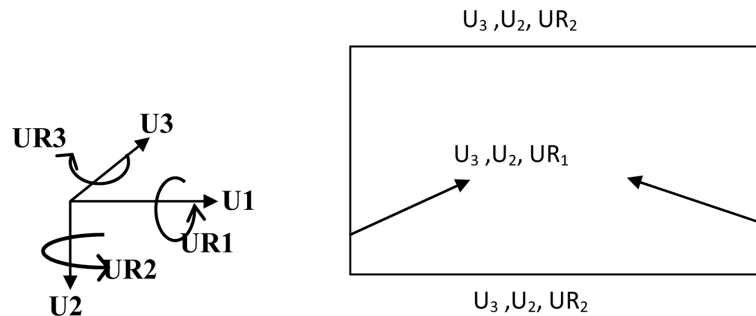


Fig. 4 Simply supported boundary condition with arrested DOF (at each of plate edges)

unchanged and exact for the case of pure shear, in all the three above boundary condition. Hence, in the present case of combined shear and tension, in-plane translational DOF, U_2 is restrained to prevent the rigid body movement. Then, the simply supported boundary (out of plane) condition is modeled by arresting appropriate DOF at each plate edges as per literature (Alinia and Dastfan 2006) and is shown in Fig. 4.

5.2.5 Meshing

In the FE procedure, the conventional stress/displacement shell element, S4R is chosen throughout the present study since it ensures that Kirchhoff's constraint (ABAQUS 6.9) is satisfied. Here 'R' denotes the reduced integration which is used in the present study to avoid the condition of 'shear locking'. The element size of 20 mm (along plate's longer edge) and an element aspect ratio of 2 are arrived, based on the convergence observed in the buckling solution, at the chosen element size in the mesh sensitivity analysis (shown in Fig. 7), that has been carried out for the case of combined shear and tension, with value for tension kept as zero. In the convergence study, the element size is chosen as parameter as against to conventional element number in order to make the convergence study independent of plate aspect ratio.

Since four sided, 2-D region with no hole and with isolated edges can be meshed with structured meshing technique, as it provides most control over the mesh that ABAQUS generates (ABAQUS 6.9), the same meshing rule is adopted all through the numerical modelling of the present study.

5.3 Validation of FE procedure

For the purpose of validating the proposed FE procedure (as mentioned in Sec. 5.2), it is applied to the standard case of combined shear and compression and it is found to give same buckling load (see Fig. 6) as that of literature (Galambos 1998) and it also captures the exact buckled mode shape as shown in the literature (Stein and Neff 1947), for all possible load combinations at buckling and is shown in Fig. 5. With this validation, the FE procedure/modeling as mentioned in section 5 (also shown in Table 1) is adopted for shear and tension. The intersection of the curve in the Fig. 6 at X -axis and at Y -axis validates the adopted FE procedure for the case of pure compression and pure shear respectively.

The results of buckling analysis of plate subjected to combined shear and tension, obtained through both analytical method and numerical modeling are presented and compared in the following section.

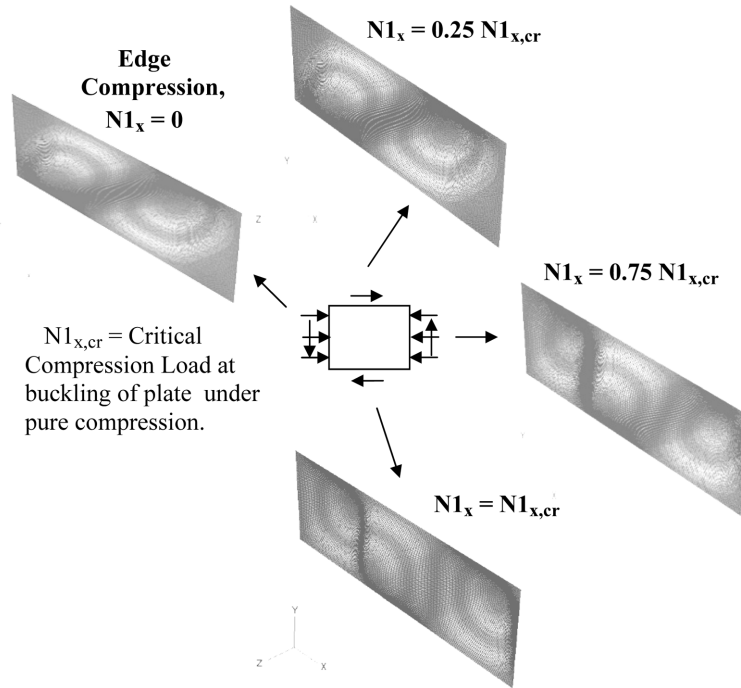


Fig. 5 First mode of plate under varying axial compression (N_{1x})

Table 1 FE procedure/modeling adopted for the validation and then to plate under combined shear and tension

S.No	ABAQUS-Module	Parameter	Values	Units
1	Part Module	Plate aspect ratio	1 to 5	
2		b/t	166	$b = 1 \text{ m}, t = 6 \text{ mm}$
3	Property Module	Modulus of elasticity, E	2.10E+05	N/mm ²
4		Poisson's ratio	0.3	
5		Boundary condition (for both step 1 & 2)	Simply supported on all its edges	*Edge along X-axis: U3,U2,UR2-arrested
6	Multistep Buckling Analysis			*Edge along Y-axis: U3,U2,UR1 -arrested
7		Load Module	In this, the plate model is loaded using shell edge load – Normal edge traction for tensile/compressive load in step 1 (General static step) and by shell edge load – shear edge traction for shear load in step 2 (Buckle step), by selecting the respective geometric edges as a load application area.	
8				
9		Element type	S4R	
14	Mesh Module	Meshing Rule	Structure Meshing	
15		Element size, along plate's long edge	20	mm

*Here U, UR refers to translation and rotational displacement respectively and 1,2,3 refers to X, Y, Z axis respectively, with plate lying in XY plane (Refer Fig. 2)

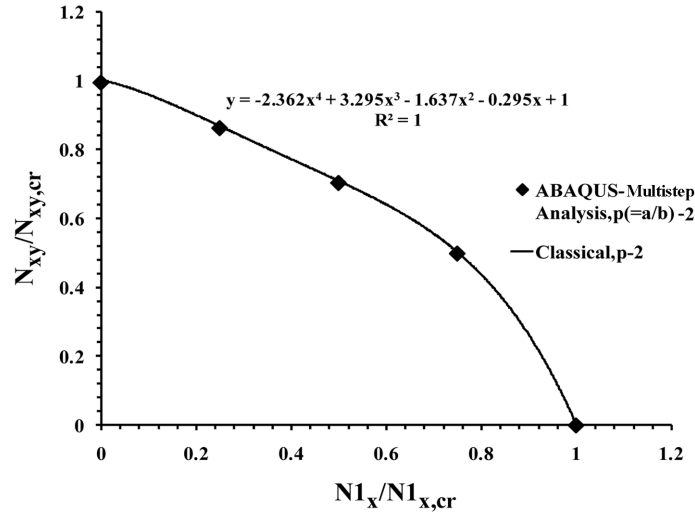


Fig. 6 Validation of multistep buckling analysis for $p = 2$ - Combined shear (N_{xy}) and compression ($N1_x$) load case

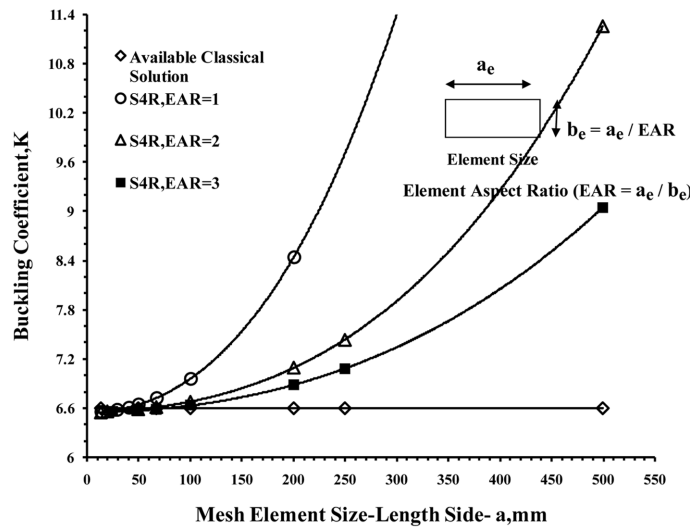


Fig. 7 Convergence study for choosing mesh element for the case of pure shear

6. Results and discussions

The results (interaction curve) of buckling analysis of plate under combined shear and tension are presented in the Figs. 8, 9. The buckling mode shape of plate of various aspect ratio (1 to 5) are also found to be in good agreement with that of pure shear case (Stein and Neff 1947). With this, it is observed from the results (both buckling load and corresponding mode shape) of numerical modelling that experimental observation of delayed shear buckling as reported in the literature (Baskar and Shanmugam 2003) is satisfied, which inturn validates the use of adopted FE procedure

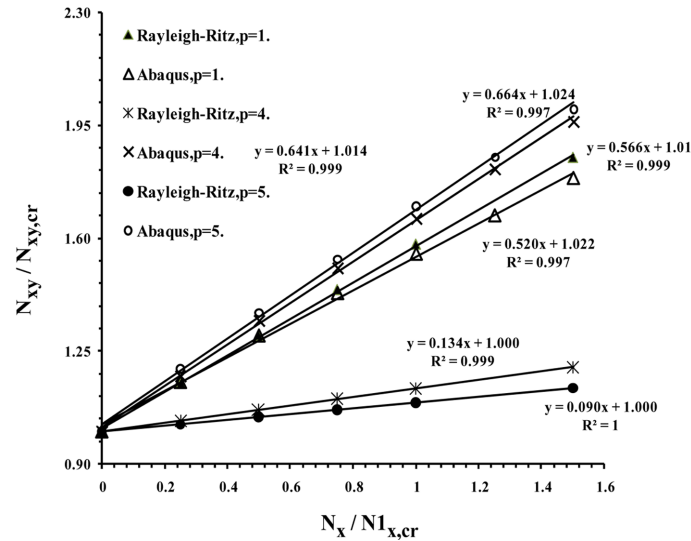


Fig. 8 Buckling interaction curve for combined shear (N_{xy}) and tension (N_x), for plate of aspect ratio, $p = 1, 4$ & 5

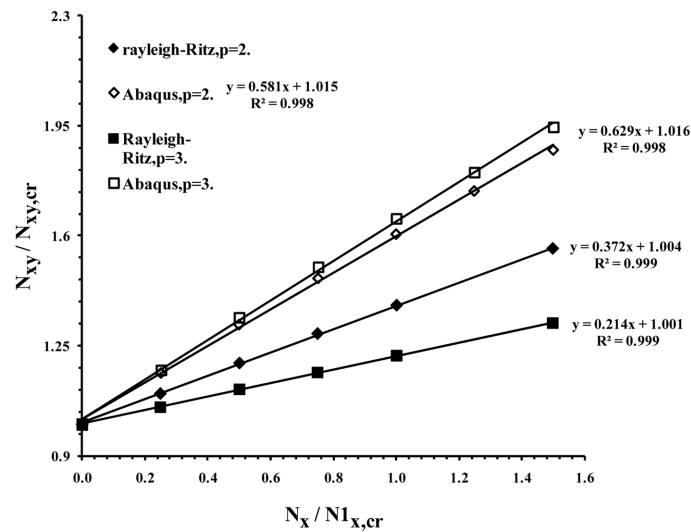


Fig. 9 Buckling interaction curve for combined shear (N_{xy}) and tension (N_x), for plate of aspect ratio, $p = 2, 3$

for the case involving combined shear and tension. Hence, the results of numerical method is taken as datum for the following discussion.

The increase in plate shear load at buckling, under the combined action of shear and tension with respect to that of pure shear case is found to increase with increase in plate aspect ratio for any given tension load. An increase of 29.8%, 31.7%, 34.2%, 34.5% and 37.1% is observed at the chosen tension load value of $0.5N_{1x,cr}$, for the plate aspect ratio of 1, 2, 3, 4 and 5 respectively and can be seen in Figs. 8, 9. It is also observed that the buckling interaction curve for the combined shear and tension is linear and it varies as plate aspect changes and the same is shown in Figs. 8, 9.

As the accuracy in capturing the actual plate buckling profile depends on the number of terms considered in the assumed double trigonometric deflection function (i.e., buckling profile) of the energy (Rayleigh-Ritz) method (Cook *et al.* 2004, Timoshenko and Gere 1985), consideration of lesser number of terms will make it to deviate from that of actual buckling profile (Cook *et al.* 2004). This deviation will in turn decrease the accuracy of the resultant buckling solution i.e. buckling interaction curve and this formed the main reason for the observed deviation of buckling curve of Rayleigh-Ritz method (Figs. 8, 9) from that of validated Numerical modeling in the present study (Figs. 8, 9). It is also observed that for plate aspect ratio of 1, the number of terms considered in the assumed deflection expression is adequate to capture the actual plate buckling profile and hence, the results of both energy and numerical experimentation (Figs. 8, 9) are in good agreement. But this is not the case for plate aspect ratio greater than one. Deviations of 16.8%, 32%, 38.8% and 43.2% is observed at the tensile load value equals to $1.5N_{1,cr}$, for the considered plate aspect ratio of 2, 3, 4 and 5 respectively and are shown in Figs. 8, 9.

From the analysis of cases involving combined shear and compression (Fig. 6) and combined shear-tension (Figs. 8, 9), it is found that shortening/elongation of the plate's longitudinal fiber decreased/increased the shear load at buckling respectively.

In the further study of the present case of combined shear and tension, number of terms to be considered in the assumed deflection expression of Rayleigh-Ritz method, is to be evaluated through convergence study (i.e., checking the convergence of Rayleigh-Ritz solution by considering more number of terms in the deflection profile, in each case) in order to predict the exact deviation between the buckling solution of analytical and numerical model. If deviation exists, the reason for such deviation is to be evaluated.

7. Summary

Based on the detailed study carried out in the buckling analysis of Kirchhoff plates (Un-perforated) under the combined action of shear and tension, the following summary and conclusions are arrived.

1. Buckling characteristics of Kirchhoff plate under the combined action of shear and tension is found to be a delayed shear buckling, as reported in the literature (Baskar and Shanmugam 2003), as experimental observation.
2. In single step analysis, since it is not possible to get shear load at buckling for the given tensile/compression, the multi step analysis is proposed and used to arrive at the shear load at buckling for the given tension and the interaction buckling curves are drawn.
3. In the proposed multi step buckling analysis, it is found that the shortening/ elongation of plate longitudinal fibers, produced under the action of in-plane compression/tension changed the shear load at buckling. The shortening of the fibers reduced the shear buckling whereas the elongation in the fiber increased the shear buckling load i.e. caused a delayed shear buckling. Thus, it is found that the elongation developed due to the presence of tensile force is inducing a stabilizing effect, which in turn delays the shear buckling.
4. The transition of buckling mode shape in the case of combined shear and compression, from pure shear to pure compression is well captured in the present study, with the use of multi step buckling analysis.

8. Conclusions

1. The buckling interaction curve for combined shear and tensile case is found to be linear and it depends on plate aspect ratio. The presence of in-plane tensile force increased the shear load at buckling in comparison to that of pure shear case, for plates of all considered plate aspect ratios.
2. The increase in plate shear load at buckling, with respect to that of pure shear case, under the combined action of shear and tension case, is found to increase with increase in plate aspect ratio for any given tension load. An increase of 29.8%, 31.7%, 34.2%, 34.5% and 37.1% is observed at the chosen tension load value of $0.5N_{1x, cr}$, for the plate ratio of 1, 2, 3, 4 and 5 respectively.
3. In the case of square plate (i.e., plate with aspect ratio = 1), the buckling interaction curve is in good agreement with that of numerical experimentation and hence the number of terms (corresponding to $m, n, r, s = 1, 2$) considered in the assumed double trigonometric deflection function (i.e., buckling profile) of the energy method, is adequate in capturing the actual plate buckling profile.
4. In the case of rectangular plates with aspect ratio greater than 1, the buckling interaction curve of Rayleigh-Ritz method is found to be deviating from that of validated numerical modeling. It is due to the fact that the number of terms considered in the assumed buckling profile of the energy method is inadequate to capture the actual buckling profile and this resulted in the decay in the accuracy of its buckling solution, which in turn resulted in the observed deviation.
5. The observed deviation in the analytical buckling interaction curve from that of numerical is found to increase with increase in plate aspect ratio at any given tensile load. A deviation of 16.8%, 32%, 38.8% and 43.2% is observed at the tensile load value equals to $1.5N_{1x, cr}$, for the considered plate aspect ratio of 2, 3, 4 and 5 respectively. Also, the deviation is found to increase with increase in in-plane tension for the chosen plate aspect ratio.

References

- Alinia, M.M. and Dastfan, M. (2006), "Behavior of thin steel plate shear walls regarding frame members", *J. Constr. Steel Res.*, **62**, 730-738.
- Alinia, M.M., Gheitani, A. and Erfani, S. (2009), "Plastic shear buckling of unstiffened stocky plates", *J. Constr. Steel Res.*, **65**, 1631-1643.
- Bulson, P.S. (1970), *The Stability of Flat Plates*, Chatto & Windus, London.
- Brown, C.J. and Yettram, A.L. (1986), "The elastic stability of square perforated plates under combinations of bending, shear and direct load", *Thin Wall. Struct.*, **4**, 239-246.
- Brown, C.J., Yettram, A.L. and Burnett, M. (1987), "Stability of plates with rectangular holes", *J. Struct. Eng.*, **113**(5), 1111-1116.
- Baskar, K. and Shanmugam, N.E. (2003), "Steel-concrete composite plate girders subject to combined shear and bending", *J. Constr. Steel Res.*, **59**, 531-557.
- Chandrashekhara, K. (2001), *Theory of Plates*, 1st Ed., University Press, India.
- Cook, R.D., Malkus, D.S., Plesha, M.E. and Witt, R.J. (2004), "Concepts and applications of finite element analysis", 4th Ed., Wiley, India.
- Chen, Y.Z., Lee, Y.Y., Li, Q.S. and Guo, Y.J. (2009), "Concise formula for the critical buckling stresses of an elastic plate under biaxial compression and shear", *J. Constr. Steel Res.*, **65**, 1507-1510.
- Elbridge Z. Stowell and Edward B. Schwartz (1943), "Critical stress for an infinitely long plate with elastically restrained edges under combined shear and direct stress", NACA - Advance Restricted Report No :3X13.
- EL-Sawy, K.M. and Nazmy, A.S. (2001), "Effect of aspect ratio on the elastic buckling of uniaxially loaded

- plates with eccentric holes”, *Thin Wall. Struct.*, **39**, 983-998.
- EL-Sawy, K.M. and Martini, M.I. (2007), “Elastic stability of bi-axially loaded rectangular plates with a single circular hole”, *Thin Wall. Struct.*, **45**, 122-133.
- Galambos, T.V. (1998), *Guide to Stability Design Criteria for Metal Structures*, 2nd Ed., John Wiley, Newyork.
- IS:11384 (1985), *Code of Practice for Composite Construction in Structural Steel and Concrete*, Bureau of Indian Standards, India.
- Iyengar, N.G.R. (1986), *Structural Stability of Columns and Plates*, East-West Press, India.
- Jaberzadeh, E. and Azhari, M. (2009), “Elastic and inelastic local buckling of stiffened plates subjected to non-uniform compression using the Galerkin method”, *Appl. Math. Model.*, **33**, 1874-1885.
- Lee, S.C., Davidson, J.S. and Yoo, C.H. (1996), “Shear buckling coefficients of plate girder web panels”, *Comput. Struct.*, **59**(5), 189-795.
- McKenzie, K.I. (1963), “The buckling of a rectangular plate under combined biaxial compression, bending and shear”, *The Aeronautical Quarterly*, August.
- Maiorana, E., Pellegrino, C. and Modena, C. (2009), “Elastic stability of plates with circular and rectangular holes subjected to axial compression and bending moment”, *Thin Wall. Struct.*, **47**, 241-255.
- Moen, C.D. and Schafer, B.W. (2009), “Elastic buckling of plates with holes in compression or bending”, *Thin Wall. Struct.*, **47**, 1597-1607.
- Narayanan, R. and Der Avanessian, N.G.V. (1984), “Elastic buckling of perforated plates under shear”, *Thin Wall. Struct.*, **2**, 51-73.
- Naik, R.T. and Moen, C.D. (2009), “Elastic buckling studies of thin plates and cold-formed steel members in shear”, Research Article.
- Paik, J.K. and Thayamballi, A.K. (2000), “Buckling strength of steel plating with elastically restrained edges”, *Thin Wall. Struct.*, **37**, 27-55.
- Paik, J.K. (2007), “Ultimate strength of perforated steel plates under edge shear loading”, *Thin Wall. Struct.*, **45**, 301-306.
- Pellegrino, C., Maiorana, E. and Modena, C. (2009), “Linear and non-linear behavior of steel plates with circular and rectangular holes under shear loading”, *Thin Wall. Struct.*, **47**, 607-616.
- Stein, M. and Neff, J. (1947), “Buckling stresses of simply supported rectangular flat plates in shear”, NACA: technical note-1222.
- Shahabian, F. and Roberts, T.M. (1999), “Buckling of slender web plates subjected to combinations of in-plane loading”, *J. Constr. Steel Res.*, **51**, 99-121.
- Shimizu, S. (2007), “Tension buckling of plate having a hole”, *Thin Wall. Struct.*, **45**, 827-33.
- Timoshenko, S.P. and Gere, J.M. (1985), *Theory of Elastic Stability*, 2nd Ed., McGraw Hill, Singapore.
- Xiang, Y., Wang, C.M., Wang, C.Y. and Su, G.H. (2003), “Ritz buckling analysis of rectangular plates with internal hinge”, *J. Eng. Mech.-ASCE*, **129**(6), 683-688.
- Yettram, A.L. and Brown, C.J. (1985), “The elastic stability of square perforated plates”, *Comput. Struct.*, **21**(6), 1267-1272.
- Yettram, A.L. and Brown, C.J. (1986), “The elastic stability of square perforated plates under biaxial loading”, *Comput. Struct.*, **22**(4), 589-594.
- ABAQUS, ABAQUS/Standard Version 6.9, Set of User and Reference Manuals, Dassault Systèmes, Simulia Corp., Providence, RI, USA.

Notations

a	: Length of the plate
a_e	: Size of mesh element along plate's longitudinal edge
A_{ij}	: Constant coefficients in assumed deflection function of Rayleigh-Ritz method, where $i, j = 1, 2, 3, \dots, n$.
A_s	: Cross sectional area of steel beam of a composite section
b	: Width of the plate
b_e	: Size of mesh element along plate's transverse edge
b_{eff}	: effective width of flange of slab
dx	: Differential chord length of plate
ds	: Differential buckled plate curve length
dl	: Differential displacement of the plate loaded edge due to applied in-plane load
d_c	: Vertical distance between centroids of concrete slabs and steel beam in a composite section
d_s	: Depth of concrete slab of a composite section
D	: Flexural rigidity of plate
E	: Elastic modulus of the plate
$(f_{ck})_{cu}$: Characteristic (cube) compressive strength of concrete
f_y	: Yield strength of steel
F_{cc}	: The total compressive force in concrete
K	: Buckling coefficient
K_o^{MN}	: Stiffness matrix corresponding to base state
K_{Δ}^{MN}	: Differential initial stress and load stiffness matrix
m, n, r, s	: Integer counts for denoting each terms of deflection function, $w(x, y)$
M, N	: Degree of freedom of the whole plate model
NI_x	: In-plane compressive load in x direction
N_x	: In-plane tensile load in x direction
$NI_{x,cr}$: In-plane critical compressive load at buckling for the case of pure compression
N_{xy}	: In-plane shear load
$N_{xy,cr}$: In-plane critical shear load at buckling for the case of pure shear
$p (= a/b)$: Plate aspect ratio
P^N	: Preload of ABAQUS Buckling step
Q^N	: Load given in ABAQUS Buckling step
t	: Thickness of plate
U	: Strain energy of the loaded plate
$U1, U2, U3$: Translational DOF in X, Y, Z axis direction respectively
$UR1, UR2, UR3$: Rotational DOF in X, Y, Z axis direction respectively
V_e	: Potential energy due to external load system
V_i	: i th Eigen vector i.e., Buckled mode shape
V_1	: Potential energy due to tensile load
V_2	: Potential energy due to in-plane shear
$w(x, y)$: Deflection (out of plane) function
x_u	: Depth of neutral axis at ultimate limit state of flexure
λ_i	: Eigen Value of i th mode shape (i.e., Eigen vector)
γ	: Poisson's ratio of plate
x, η	: Non dimensional parameters of Rayleigh-Ritz method
π	: Total potential energy of the system

Abbreviation

CLDM	: Conjugate Load/Displacement Method
DOF	: Degrees of Freedom
EAR	: Element Aspect Ratio
FE	: Finite Element
FEM	: Finite Element Method
PE	: Potential Energy
2-D	: Two dimensional